Rev. Adv. Mater. Sci. 51 (2017) 62-76

MACHINING PROCESSES OF SILICON CARBIDE: A REVIEW

P. Pawar, R. Ballav and A. Kumar

Department of Manufacturing Engineering, National Institute of Technology, Jamshedpur, 831014, Jharkhand, India

Received: May 16, 2017

Abstract. Silicon Carbide (SiC) is an inorganic material having mechanical, thermal, electrical and chemical properties, due to which it is widely used in developed industries. However, the beneficial properties of SiC ceramic such as high hardness, high strength, wear resistance, extreme brittleness and chemical stability make SiC machining difficult and costly through conventional and non-conventional machining methods. Hence, in present study an overview of previous work on SiC ceramic is carried out. Many researchers attempted various methods for machining of SiC ceramic from which electro discharge machining process, laser machining process, grinding process and diamond turning machining process is the most applied methods. The theoretical, experimental and simulation studies are considered for obtaining significant results. The researchers mainly focused on Material removal rate, surface roughness, surface finish and tool wear rate.

1. INTRODUCTION

The Silicon Carbide (SiC) is a compound containing two elements i.e. silicon (Si) and carbon (C). The mixture of silicon with carbide is termed as Moissanite which is discovered by H. Moissan (1893) on meteorite rock in Diablo Canyon, Arizona [1]. E. G. Acheson (1891) created silicon carbide in the laboratory and termed as Carborundum [1-3]. Silicon carbide is the fourth hardest material in the world [2]. The forms of SiC used for commercial purposes are single crystal, polycrystalline and amorphous [3]. According to the National Aeronautics and Space Administration agency (NASA), USA the silicon carbide has to be considered as future material, which can be used in semiconductor electronic devices [4].

The mechanical properties of SiC are high hardness, wear resistance, high durability, light weight, extreme brittleness, poor machinability, low density, high rigidity, excellent corrosion resistance, high strength, high specific stiffness, high intensity and high toughness [2,3,5-11,13-25,28-35]. The thermal properties of SiC contain high thermal shock resistance, thermal stability, low thermal distortion, low thermal coefficient expansion, radiation resistance, high thermal conductivity and low activation [2,6-12,14,16,17,19-23,25-32,34,35]. The low conduction electricity, electromagnetic response, wide energy band gap, high breakdown voltage, strong covalent bonding and high carrier mobility are the electrical properties of SiC [2,10, 12,20,22,24,26,27,30,31,33]. The SiC have different chemical properties i.e. high oxidation, low toxicity, chemical stability, chemical resistance, chemical inertness and biocompatibility [5,6,10,11,13-15,20-25,28,30-35].

The SiC is mostly applicable in industrial, defense, electrical and electronics technologies, automobile industries, aerospace technologies and biomedical fields. In industrial areas it is used as furnace heating elements, petrochemical industries, cutting tools, mechanical seals, high-temperature

Corresponding author: P. Pawar, e-mail: pravin.1900@gmail.com

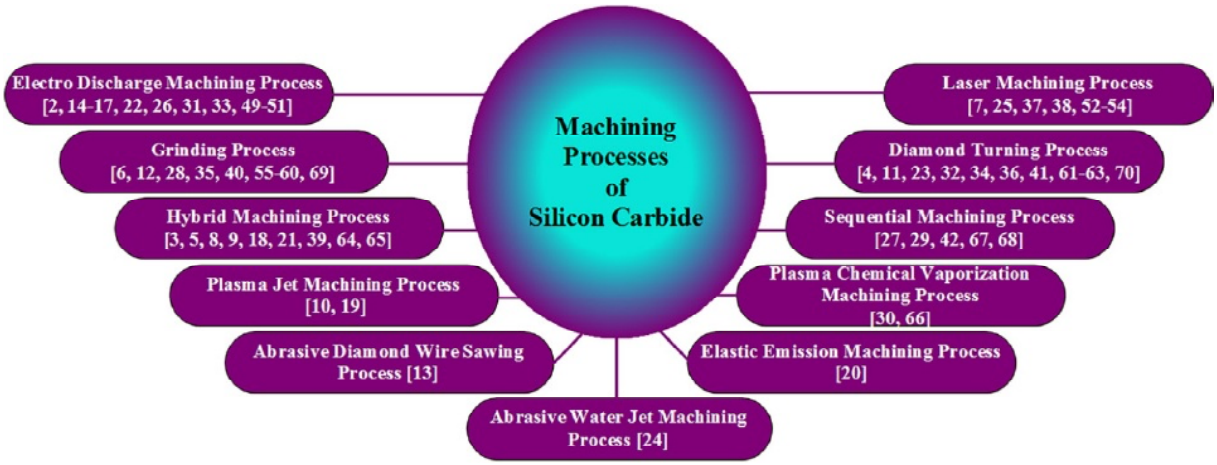

Fig. 1. Machining processes of Silicon Carbide.

bearings, valves, fixtures, turbine blades, heat exchangers, corrosion resistant containers, pipes in oil industry, dies, refractories, centrifuge tiles and textile thread guides [2,4,6-8,14-18,22,24,31,34-36,39-41]. Whereas, in the field of defense it is applicable in atomic centers as protector, composite armor protection, military aircraft, ballistic armor, laser radar systems, the regulator of neutrons and combat vehicles [2,4,22,23,31,36]. In electrical and electronics technologies it is used in power generation, high current AC/DC converter system, quantum computing applications, heavy-duty electric contacts, electronics, optical mirror, nose covers in Airborne laser devices, light emitters and high power electronics [4,6,8,10,14,16,17,23,26,35,36,39,41]. In automobile field, it is applicable for automotive engine components, rotors, nozzles, composite automotive brakes, automotive water pumps, accelerometer, stators, and diesel particulate filters [6-8,14-17,22,24,31,39,40]. In the aerospace technologies, SiC utilized for space-born mirrors, weather satellites, vacuum ultraviolet telescopes, and aerospace applications [10,14,23,39,42]. It is also advantageous in the biomedical field for bioengineering, C/C complex material in biomedicine, micro electromechanical systems (MEMS), micro sliders and biomedical applications [6,7,13,14,16,26,37-39].

The SiC got prime importance in different commercial areas, but it has long machining time, lower production rate with high tool wear which causes higher machining cost [5,6,8,13,14,16-20,22,25]. There are different types of SiC machining processes i.e. ultrasonic machining process, diamond tool machining process, plasma chemical vaporization machining process, electrical discharge machining process, laser beam machining process, etc. [39]. H. Abderrazak et al. [43] described the different methods used for the elaboration of SiC are chemical vapour deposition, liquid phase sintering, physical vapour deposition, sol-gel, mechanical alloying. The physical vapour deposition technique is mostly applicable to produced crystalline materials like semiconductors. M. Wijesundara et al. [44] reviewed on SiC materials with reference to technologies used to manufacture SiC electronics, micromechanical transducers, and packaging. Y. Pachaury et al. [45] reviewed on EDM process to machine different ceramic materials such as ZnO_2, Si_3N_4, Al_2O_3, SiC, and their composites. Also, A. Samant et al. [46] given a review on laser machining process of structural ceramics to recognize the physical phenomenon related to the machining process. The laser process parameters and properties of material are the main reasons which form material removal rate. S. Goel [47] reviewed on detail study about how to prepare a molecular dynamics simulation and to know its significant view towards the diamond machining of SiC. C. Lauro et al. [48] concluded that for obtaining high surface quality the use of micromachining process is a great option.

The advancement in SiC machining technologies is changing vastly due to which its applicability is increasing in various fields. Hence, to take an overview of progress in SiC machining process the present work has to be undertaken.

2. MACHINING PROCESSES OF SILICON CARBIDE

There are different types of machining processes used by various researchers to machine the SiC material. The 11 types of SiC machining processes which are obtained from current literature survey was presented in Fig. 1.

2.1. Electro discharge machining process

R. Mahdavinejad et al. [2] analyzed instability in electro discharge machining (EDM) of SiC which is an effect of heat generation in the workpiece. They found that the voltage drop produces joule heating in silicon carbide body which is the main factor in the electro discharge machining process. R. Ji. et al. [14] invented a new technique having a group pulse power supply for electric discharge (ED) milling of SiC with a resistivity of 500 Ωcm. The results show that the most suitable parameters for SiC machining are smaller high-frequency pulse duration, pulse interval, peak current, higher peak voltage, and positive tool polarity. This method provides good machining stability and high pulse utilization which causes the material removal rate (MRR) up to 72.9 mm^3/min. R. Ji. et al. [15] estimated a new process in which they used water based emulsion as machining fluid which resulted in to high efficiency and good conditions during environmental practices. From the obtained results, they found lower electrode wear rate and higher MRR both having negative polarity. R. Ji. et al. [16] also concluded that the MRR and tool wear rate both are increases with increasing in emulsion flux, whereas the increase in emulsion flux causes the reduction in surface roughness. R. Ji. et al. [17] machined a large surface area on SiC by using a steel-toothed wheel in electric discharge milling process. To find out the best machining fluid emulsion in this process they compared three types of machining fluid. The observations show that a water-based emulsion did not produce harmful gases during machining and it gives good working conditions during environmental practices. They found many craters and grains on the surface of machined SiC ceramic with emulsion 1. Whereas, in a case of emulsion-2 the craters and grains quantity was very small as compared to emulsion 1. In emulsion-3 the smooth machined surface of SiC was found which was covered by craters and grains. Y. Liu et al. [22] achieved high MRR and better surface quality in ED milling process by using a steel-toothed wheel as tool electrode. Y. Zhao et al. [26] experimentally investigated EDM performances on SiC by using copper foil as electrode tool and compared with steel electrode tool material. For copper foil EDM of SiC, the negative polarity is more suitable which gives higher machining speed with lower tool wear ratio. From the observations, they concluded that the use of thinner foil as an electrode having increasing discharge current helps to improve the cutting speed of foil EDM for SiC.

Y. Liu et al. [31] have machined SiC material by using ED milling process. For this analysis, they applied a steel-toothed wheel which worked as tool electrode. This process can improve hardness, MRR, mechanical character and surface quality. T. Kato et al. [33] found that, as compared to diamond sawing the EDM process showed excellent results for high efficiency and high precision having low damage machining for the single crystals of SiC. C. Luis et al. [49] examined MRR and electrode wear of reaction-bonded SiC. The most influencing parameters for MRR are intensity and voltage. Whereas, the wear rate was affected by intensity, pulse time and flushing pressure. F. Zeller et al. [50] invented two approaches in the EDM process by using assisting electrode i.e. adaption of tool geometry and adaption of process parameters. They observed in the adaption of process parameters, drilling depth obtained up to 150 μm, however in the adaption of tool geometry maximum depth achieved up to 420 μm. The combination of both approaches increases the accuracy of depth and the machining time. The maximum MRR was reached up to 3.58 × 10^{-3} mm^3/min. S. Yamaguchi et al. [51] used EDM process and adapted a new method for the cutting of SiC ingots and slabs. For keeping higher electric conduction during the experiments they used three methods i.e. photoconductive, high electric field effect and high-temperature effect. The cutting rate of this process is 1000 times greater than the ordinary EDM and 10 times higher than diamond saw.

2.2. Laser machining process

Y. Aono et al. [7] established silicon elimination based method named as the carbide-derived carbon process. For the local modifications performance, they used amorphous thin films and sintered polycrystalline plates. The infrared laser with or without pre-heating was used which creates modified layers on both the specimens. The obtained result shows that the purity, thickness of the layers and chemical bonding continuity depends on the laser irradiation situation, which caused by ablation. Q. Zhang et al. [25] observed that the edge and wall of the holes both are covered by small particles having waviness. The increase in laser energy density simultaneously decrease in depth of holes was observed and the hole diameter showed slightly change. D. Duc et al. [37] predicted absorption coefficient (2.5x10^5 m^{-1}) and ablation threshold (7.8 J/cm^2) for SiC in laser drilling process. They observed

free carriers absorption for Absorption mechanism of solid SiC in infrared wavelength regime which is mainly dependent on temperature. N. Iwatani et al. [38] used ns pulsed infrared Nd: YAG laser to investigate the effects of underwater laser drilling process of silicon carbide wafer. They observed increasing via diameter, reducing etching rate and generation of cracks in the high-energy regime and it can create vias which don't have heat affected zone, debris, and cracks.

A. Samant et al. [52] developed a theoretical model that includes thermal effects in decomposing material, surface tension in expelling molten part, the effect of evaporation-induced recoil pressure, loss in energy and cooling of the surface. According to them these all are responsible for the formation of the hole. Also, this model can provide an approximate pulses number which was required for drilling at the desired depth in given material. I. Shigematsu et al. [53] investigated laser machining of SiC by using N_2, O_2, and air as the medium. The results showed that the metallic silicon particles remained on the machined surface. The generation of toxic gases takes place during machining and as result; the ultra-fine SiO_2 powder was produced. D. Sciti et al. [54] used an inert atmosphere to avoid surface oxidation during a KrF excimer laser machining process. They observed melting of surface and resolidification occurred at low fluence. However, at high fluence due to vaporization, the material removal occurred. Therefore, SiC surface shows a rugged morphology without cracks.

2.3. Grinding process

S. Agarwal et al. [6] applied the diamond grinding wheel to analyze the maximum removal rate of SiC grinding. They observed that due to the micro fracture and grain dislodgement, the MRR gets improved which did not effect on the surface morphology and surface finish. A. Gopal et al. [12] assessed SiC grinding performance by a newly invented model which has chip thickness. A new model includes material properties of wheel and workpiece. The verification of new model is done by taking surface roughness as a parameter. According to them, as compared to existing models, a new chip thickness model gives good accuracy for predicting the surface roughness. Y. Wang et al. [28] used surface milling machine for grinding reaction bonded silicon carbide (RB-SiC) with the help of diamond wheels. They found that the increase in depth of cut also raises the surface roughness. Whereas, when the burnishing time increases, the surface roughness gets reduces. As the depth of cut increases simultaneously, increase in subsurface damage was observed, which resulted in reduction of hardness. L. Yin et al. [35] used CNC grinding machine to obtain a high quality grinding structure on SiC material. They obtained surface roughness 9.92-17.22 nm and observed that the low machining induced damage caused due to microstructural defects such as pores. N. Padture et al. [40] observed that microstructural heterogeneity noticeably improves the drilling and grinding rates of SiC. The residual machining damage observed on machined surface which shows low strength for heterogeneous material. A. Gopal et al. [55] examined SiC grinding process by using genetic algorithms optimization technique which resulted in the maximum MRR, surface finish, and damage. The output responses surface roughness and damage are influenced due to the effect of wheel grit size, work feed rate and depth of cut. B. Groth et al. [56] machined SiC surface shows that the presence of compressive residual stresses on surface and subsurface region of hot-pressed SiC resulted into lowest surface roughness and mirror like finish. Y. Liu et al. [57] combined Johnson-Holmquist 2 damage model and the Griffith fracture theory model to establish the dynamic fracture toughness of SiC in a high-speed grinding process. According to them, the dynamic toughness of the SiC in the high-speed grinding process influenced by hydrostatic pressure, strain rate and material damage degree. The SiC dynamic fracture toughness enhanced by an elevated wheel surface speed, which can achieve high MRR having a better surface finish. Z. Zhong et al. [58] obtained high shape accuracy and low surface roughness on elliptic, circular and toroidal mirrors which are made up of SiC with large curvature radii by using grinding process. D. Zhu et al. [59] investigated the initiation and propagation of individual cracks in SiC grinding using single-grit simulations. According to simulated results when maximum undeformed chip thickness is kept below 0.29 μm that time the material removal is dominated by the ductile regime grinding. However, when maximum undeformed chip thickness exceeds up to 0.3 μm that time the brittle removal mode becomes more significant which forms transverse cracks. J. Ni et al. [60] observed that phase transformation can decrease by the combination of greater workpiece speed and elevated grinding wheel velocity. The result shows that polytype transitions occurred under cylindrical grinding conditions. H. Xu et al. [69] studied the machining of SiC in which they evaluated the effects of

microstructural heterogeneity on material removal mechanisms and damage creation processes. They observed that depending upon the microstructural structure of SiC, it can control material removal by grain dislodgment during machining as well as it suppresses formation of strength degrading cracks and imparting tolerance to machining damage.

2.4. Diamond turning machining process

S. Goel et al. [4] applied Single point diamond turning process with molecular dynamic simulation on single crystal β-SiC. They observed a sp^3-sp^2 order-disorder transition influenced by the high magnitude of compression in cutting zone which also influences the diamond tool wear. S. Goel et al. [11] revealed the microscopic origin of ductile regime machining of single crystal 6H-SiC in the diamond turning process. For improving the tribological performance, they used Distilled water as a coolant. They achieved a surface finish having surface roughness of 9.2 nm and wear marks on cutting tool after 1km of cutting length. X. Luo et al. [23] analyzed nanometric machinability for single crystal SiC by utilizing molecular dynamics simulation. This simulation can help to understand a quantitative and qualitative behavior of single point diamond turning of various polytypes of SiC. During machining of SiC, they observed higher thrust forces than the cutting forces, whereas in silicon the opposite remarks were recorded for the same cutting condition. Z. Zhang et al. [32] observed flank wear surface consist of two areas having different wear patterns i.e. periodical microgrooves and non-periodical scratch marks. As the cutting distance increases, the non-periodical scratch marks may disappear. The microgrooves are oriented along the cutting direction. According to them, the tool swinging cutting method can remarkably improve the performance of the tool and considerably reduces the tool wear. J. Yan et al. [34] machined RB-SiC ceramics by using large-radius round- nosed diamond tools to investigate the mechanism for material removal. The machined surface roughness is mainly dependent on the tool rake angle and does not effect on the tool feed rate. The mechanism of material removal is due to cleavage cracking, ductile cutting, and grain dislodgement, which showed precision machining with a very high MRR. S. Goel et al. [36] formed SiC-graphene like substance in a cubic SiC during the nanometric cutting process using molecular dynamics simulation. They observed sp^3-sp^2 order-disorder transition of diamond tool affected by the continuous abrasive action between SiC and the diamond tool resulted in tool wear and graphitization of diamond. J. Patten et al. [41] compared experimental results of single point diamond turning of single crystal SiC with numerical simulations results achieved from AdvantEdge software. The simulations can predict the thrust and cutting forces produced in ductile cutting conditions. J. Patten et al. [61] experimented on single-crystal SiC by single point diamond turning process to find the performance ability of a ductile material removal operation. They determined the formation of a high-pressure phase at the cutting edge resulted into ductility of SiC, which includes the volume of its associated material and chip formation zone. H. Tanaka et al. [62] experimentally concluded that at a depth of cut smaller than 60 nm shows the ductile mode machining of surface-modified SiC and this result was observed without cutting edge chipping. Also, at the time of interface between the crystalline base material and an amorphous layer, the micro crack propagation obstructed. They also proved that, the damage free machining of monocrystalline SiC achieved by surface modification. Z. Zhang et al. [63] applied single point diamond turning process to analyze the precision machinability of RB-SiC. From the results, it was observed that the material removal mechanism includes the intergranular micro-fractures of bonding silicon and falling of the SiC grains which prevents the large scale cleavage fractures. They also concluded that to get high efficiency machining results of RB-SiC the single point diamond turning process can be the best option. B. Bhattacharya et al. [70] analyzed the scratching tests for single point diamond turning simulation by using styli and single point diamond tools. According to them it is possible to achieve a surface roughness less than 60 nm by using ductile regime single point diamond turning of chemically vapor deposited coated SiC.

2.5. Hybrid machining process

The hybrid machining process is a combination of two or more processes such as laser assisted machining process, end electric discharge milling and mechanical grinding, ultrasonic vibration-assisted grinding and carbon nanofiber assisted micro electro discharge machining process are used to machined silicon carbide. D. Ravindra et al. [3] analyzed the laser heating/thermal softening effects on ductile mode machining of SiC in laser assisted machining process (μ-LAM). They achieved results of material removal caused by a larger critical depth of cut, greater depths of cuts at less thrust forces and small

cutting forces. According to them, the μ-LAM process produces lower cutting forces, which are applicable to minimize tool wear. A. Shayan et al. [5] used μ-LAM process to perform scratching experiments on 4H-SiC. In this process, diamond cutting tool and the laser system integrated and coupled for scratching on 4H-SiC. They observed more than 50% reduction in relative hardness of workpiece material, which also shows the significant reduction in cutting forces. R. Ji et al. [8] developed a process, which includes mechanical grinding and end electrical discharge milling to machine SiC ceramics. These combined processes successfully machine a large surface area on SiC ceramic with a better surface quality. They found that during initial rough machining mode, the SiC ceramic removed by end electro discharge milling then later in finer machining mode it is removed by mechanical grinding. K. Ding et al. [9] investigated the effects of ultrasonic vibration on the tool wear by conducting conventional grinding and ultrasonic vibration-assisted grinding tests on SiC. From the result, they observed the lower and more stable grinding forces were obtained through ultrasonic vibration-assisted grinding process and also slightly rougher ground surface was observed as compared to conventional grinding process. R. Ji et al. [18] machined SiC ceramic by developed hybrid machining process which includes end electric discharge milling and mechanical grinding. By using this process, they studied the effects of machining parameters on SiC ceramic, which resulted into good surface quality as well as fine working environmental practice. According to them, the short pulse on time, positive tool polarity, and low peak current are significant parameters to obtain fine surface finish. P. Liew et al. [21] machined reaction-bonded SiC material by applying newly proposed carbon nanofiber assisted micro electro discharge machining process. According to them, the addition of nanofiber helps to enhance the MRR, electro discharge frequency, and discharge gap. It reduces the electrode tip concavity and electrode wear. It also enhances the electro discharge machinability. R. Ji et al. [39] presented a new process for machining of SiC ceramics in which they combined electrical discharge milling and mechanical grinding process. This process has an ability to machine a large surface area of SiC having good surface quality. From the experimental results, they concluded that the electrode wear rate, MRR, and surface roughness values can reach up to 20.7176%, 46.2543 mm^3/min, and 0.0340 μm respectively. S. Virkar et al. [64] investigated the effect of stress and temperature during micro laser assisted machining by using three approaches. The first approach called as normalized cutting force, which was based on the cutting forces obtained from the simulation output and represents the relative dominance of temperature and stress. The second approach defines the contribution of temperature with the help of yield strength. The yield strength was the third approach which evaluated by using the Drucker-Prager pressure yield criterion. According to them the results obtained from all these three approaches indicates parallel effects of temperature and stress on the workpiece. S. Goel et al. [65] formed the surface defect machining method for the machining of nanocrystalline beta SiC with the help of molecular dynamics simulation. They observed that surface defect machining provides reduced the shear plane angle, which helps to eases the shearing action. Also, the intermittent lowering in cutting forces, dropping stresses on cutting tool and decreased operational temperature are the causes due to which increased friction coefficient supports to the tool cutting action.

2.6. Sequential machining process

X. Chen et al. [27] machined large-diameter 6H-SiC wafers by applied cutting, lapping and polishing processes sequentially. They stated that the lapping process produces deep damage layer and great residual stresses. The mechanical polishing process reduces this damage layer and residual stresses and the smooth surface having large number of scratches was resulted. The chemical-mechanical polishing effectively removes these scratches and provide very smooth surface having 0.3 nm surface roughness. J. Johnson et al. [29] stated an approach for the formation of SiC substrate by POCO Graphite Inc. In this approach, they utilized a non-traditional process that coupled with deterministic finishing techniques established by Zygo Corporation. The manufacturing of lightweight and complex SiC substrate, the POCO Graphite Inc. has developed a process, which takes short time as compared to other SiC material processes. They observed that after final polishing, the converted SiC material was clad with chemical vapor deposition SiC which creates low surface roughness. A. Damiao et al. [42] applied pastes and diamond tools to achieve mirror substrates with flat small diameter having the flatness of λ/6 and λ/100 R_a roughness. For this work, three sequential steps used to get an optical surface i.e. curve generation, grinding and polishing. H. Tam et al. [67] produced reaction bonded SiC

optical components by using two stage fabrication processes i.e. polishing and lapping. They obtained surface roughness up to 21.6 nm by applying lapping process. Whereas, surface roughness achieved up to 10.7 nm by the polishing process. Y. Filatov et al. [68] investigated results of a theoretical and experimental study of the mechanism of polishing monocrystalline SiC. From the observations, they have concluded that the density of transfer energy, the specific energy of transfer and density of vibrational energy, these all parameters are suitable to use as criteria for machining process efficiency. According to them, the coarse polishing, pre-polishing, polishing, and nano polishing are the best-polished stages for Flat surfaces of optical and optoelectronic components.

2.7. Plasma jet machining process

I. Eichentopf et al. [10] studied the MRR of C and Si-face of 4H-SiC. For the study they have utilized helium as feed gas and CF_4 as reactive gas with the atmospheric pressure of 13.56 MHz RF excited plasma jet source. However, O_2 supplied together with the N_2 shielding gas injected peripherally and they observed that the etching rate decreases with an increase in O_2 gas flow. K. Katahira et al. [19] studied the probability of atmospheric-pressure plasma jet processing for an advanced cooling effect in SiC micro-milling process. In this study, they have made a comparison between SiC surfaces obtained after milling which was with and without application of plasma jet. From the results, they observed that the plasma jet application gives high-quality surface having 0.73 nm roughness.

2.8. Plasma chemical vaporization machining process

Y. Sano et al. [30] observed that the MRR is mostly dependent on the temperature in case of Plasma chemical vaporization machining process. They found that the MRR of SiC shows much greater temperature dependence than Si. They also found that, as etching temperature increases simultaneously increase in surface roughness of the SiC Si face observed. Whereas, the C face did not show any changes in 360 °C etching temperature. Y. Sano et al. [66] defined the SiC polishing characteristics with the help of plasma chemical vaporization machining process. According to them, the C face of SiC was etched faster than Si face. They achieved very smooth surface having high machining rate i.e. up to 0.18 mm/min.

2.9. Abrasive diamond wire sawing process

H. Huang et al. [13] examined the material removal mechanism and surface roughness of single crystal SiC. This study determined fixed abrasive diamond wire sawing of SiC. The observations show that the sawn single-crystal SiC surface contains two different areas i.e. the fractured area and ploughing striations. In sawn SiC surface during low wire speed, the more fractured area was observed. Whereas, during high wire speed the more ploughing striations sawn SiC surface was obtained. They found the normal and tangential forces are approximately proportional to the volume of material removal per length of wire.

2.10. Elastic emission machining process

A. Kubota et al. [20] studied surface removal process of SiC in which they flattened a periodic step bunched structure by using elastic emission machining. The observation shows that when the top sites on periodic step bunched structure exposed to silica powder particles resulted in increased removal depth and gives smooth surface structure.

2.11. Abrasive water jet machining process

D. Srinivasu et al. [24] used abrasive water jet machining of SiC ceramic to analyze the effects of kinetic operating parameters on kerf geometry. For this study, they have taken key kinematic operating parameters such as jet impingement angle and jet feed rate. According to them, the variation of standoff distance and abrasive particle velocity distributions on these factors the jet impingement angle is mainly dependent. Whereas, jet feed rate significantly affected on exposure time of material to jet and it increases the abrasives impact erosion capacity, which gives different erosion rates.

3. A PRECISE REVIEW ON MACHINING PROCESSES OF SILICON CARBIDE

The present study is based on experimental work carried out on SiC which precisely reviewed and presented in Table 1. The table includes 11 processes used for SiC machining with its input parameters and obtained results.

Fig. 2 shows yearly progress of research with SiC machining process from 1995 to 2016. The

Table 1. Brief overview of silicon carbide machining processes.

Sr. No.	Machining Process	Main Input Process Parameters	Results obtained
1	Electro Discharge Machining Process	Workpiece material, Tool material [2,14-17,22,26,31,33,49-51], Voltage [2,14-17,22,26,49-51], Pulse on time [2,15,16,22,31,49], Pulse off-Time [2,15,16,22,31], Peak current [2,14-17,22,26,50,51], Tool polarity [2,14,16,22,31], Machining fluid [2,14-17,22,26,31,49,50], Rotating speed [14-17,22], Pulse duration [14,17,22], High-frequency pulse interval [14,17,26], Fluid concentration [2,14,26], The number of activated transistors [2], Frequency [14,50], Feed [14], Diameter of the turntable [15,16], Generator intensity, duty cycle, dielectric flushing pressure [49], Energy, Pulse width [50], Different light-emitting diodes, Electric field [51]	Material removal rate [14-17,22,26,31,49,50], Electrode wear ratio [15,16,22,26,31,49,50], Surface roughness [15,16,17,22,31], Volume of depth, Temperature [2], Micro hardness, Surface quality [14], Machining speed [26], Efficiency, Precision, Surface damage [33], Cutting rate, Flatness [51]
2	Laser Machining Process	Workpiece material, Types of Laser [7,25,37,38,52-54], Wavelength [7,25,37,38,52,54], Fluence [7,37,38,54], Repetition rate [25,38,52], Pulse energy [25,37,38,52,54], Time [7,25,37,52], Spot diameter [7,54], Pulse duration [37,38,52,54], Depth of focus [7], RF power, Base pressure, Argon pressure Distance, Thickness, Adhesion layer [7], Energy density, Focal length [25], Pulse width, Objective lens, Beam spot size, Focus position [38], Plate thickness, Operation time, Number of Pulses, Drilling energy, Pulse width ON time, OFF time, Total ON time, Total OFF time [52], Laser Multi-mode, Continuous wave Power, Feeding speed, Focal distance, Defocus, Atmosphere [53], Frequency, Number of pulses, Sample speed under the beam and atmosphere, Beam angle of incidence [54]	Surface modification [7,54], Ablation depth [37,54], Quality of machined hole [25], Ablation threshold, Absorption coefficient [37], Etching rate, Surface quality, Crack identification [38], Developed model to predict energy and time required for drilling hole [52] Observed generation of metallic silicon Particles, Toxic gases, Ultra-fine SiO_2 powder [53], Material removal, Surface roughness [54]
3	Grinding Process	Workpiece Material, Grinding wheel material, Geometry of Wheel Grinding, Speed [6,12,28,35,40,55-60,69], Feed rate [6,12,28,35,55,69], Depth of cut [6,12,28,35,55,57,58,59,69], Coolant [6,28,35,69], Workpiece speed [35,59,60], Coolant flow speed [6], Burnishing time [28], lubricant [40], Indentation Depth, The tool average grit size, Single grit engagement [57], Cross feed velocity, Table speed [58], Undeformed chip thickness, Temperature on cutting edge, Normal pressure per grit,	Surface roughness [6,12,28,35,55,56,58,59], Material removal rate and mechanism [28,40,55,57,59,69], Surface quality [28,57,59], Grinding force [6, 57], Specific removal rate [6], Generation of spherical profiles, form accuracy, wear mechanisms of tools [35], Grinding depth [40], Number of flaws [55], Shape accuracy [58] Initiation and propagation of individual

		Grit-workpiece engagement time [60], Table speed [69]	cracks in SiC grinding, Surface integrity [59], Phase transformation, residual stresses [60], Machining-induced damage on strength [69]
4	Diamond Turning Machining Process	Workpiece material, Tool material, Tool dimension, Cutting Speed, Rake angle [4,11,23,32,34,36,41,61,62], Feed rate [11, 32,34,41,62,63], Depth of cut [32,34,61, 62,63], Tool nose radius [4,11,36,61,62], Clearance angle [4,11,36,62], undeformed chip thickness [4,23,32,34,36,63], Equilibration Temperature [4,23,36], Time step [4,23,36], Cutting edge radius [11,23], Tool orientation, Cutting direction [23,36], Cutting environment [32,34], Nos. of β-silicon carbide, (cubic) Atoms in the workpiece, Nos. of diamond atoms in the tool [4], Maximum critical depth of cut [11], Maximum critical chip thickness, Coolant [11], Equilibrium lattice parameters, Crystal orientation of diamond tool [23], Cubic Crystal orientation, Cutting distance, Tool-swinging speed [32], Relief angle [34], Dimensions of SiC, Numbers of β-SiC atoms, Numbers of carbon atoms cutting Tool, Workpiece machining surface, No. of cuts [63]	Tool wear [4,11,23,32,34, 36], Cutting forces [11,41,61,23], Material removal behavior and rate [11,34,61,63], Surface roughness [11,34], Thrust force [41,61], Chip formation [11], Cutting hardness, Surface finish [23], flank wear, Wear mechanism, Cutting performance of the tools [32], Phase transformation, Large-scale fractures [34], Nanometric cutting [36], Force rate, Surface quality [61], Damage-free machining [62], Surface topography and cutting force [63]
5	Hybrid Machining Process	Workpiece Material, Tool Material [3,5,8,18,21,39,64,65], Voltage [8,18,21, 39], Current [8,18,21,39], Tool Polarity [8,18,21,39], Rotational speed, Machining fluid [8,18,39,21], Laser power, Loading, Machining condition [3,5], Cutting speed [3,5,9], Depth of cut [3,9], Feed Rate [3,9,21], Pulse On time, Pulse Off time [18, 39], Coefficient of friction [3], Pulse duration, Pulse interval, Diamond grit size, Emulsion concentration, Emulsion flux, Milling depth, Tool stick number [8], Frequency, amplitude, Coolant, coolant pressure, Grinding wheel size, material [9], Abrasive sticks size, The grit size of abrasive, Sticks diameter of the turntable [18], Condenser capacitance, Carbon nano fibers Concentration, Machining time, Cavity depth [21],Cutting edge radius, Rake angle, Relief angle, Width of tool, Length of cut [64], Equilibrium lattice parameters, Details of surface defects, Total number, Diameter of each hole, Depth of each hole, Crystal orientation of the workpiece, Crystal orientation of diamond tool, Cubic Cut-	Material removal rate [3,8,18, 21,39], Surface roughness [8,9, 18,21,39], Electrode wear ratio [8,21,39], Thrust Force, Cutting Force [3,5,64], Depth of Cut [3,5], Temperatures, Pressure [3,64], Surface integrity [18,21], Surface morphology [18,21], Width of scratch [5], Tool wear, Grinding forces [9], Composition of machined surface [18], Electrode Geometry, Spark gap, Surface damage [21], Chip Formation [64], Developed surface defect machining method using MD simulation, Improve machiniability, Reduce average cutting force [65]

		ting direction, Cutting edge radius, Uncut chip thickness/in-feed, Cutting tool rake and clearance angle, Equilibration temperature, Hot machining temperature, Cutting velocity, Time step [65]	
6	Sequential Machining Process	Workpiece material [27,42,29,67,68], Lapping tool material, Lapping speed, Abrasive material, Abrasive Size, Polishing Tool material, Polishing tool speed [27,67], Chemical [27,42], Pressure, grit size, polishing slurry material [27], Polishing time [67,42], Magnetorhelogical finishing platform wheel Size, material, MR Fluid Ribbon Height, Insertion Depth [29], Grinding wheel tool material, Tool size, Tool speed, workpiece rotation [42], scaif Speed, workpiece to tool contact pressure, crosshatch line shift, crosshatch line length, Mean temperature, polishing powder [68]	Material Removal Rate [27,29,67,68], Surface roughness [27,29,42,67,68], Efficiency [67], Flatness [42]
7	Plasma Jet Machining Process	Workpiece material [10, 19], RF excited plasma jet (CF_4, O_2, He, N_2), Power, Working distance, Diameter of the nozzle, Sample temperature [10], Plasma gas, Nitrogen Gas pressure, Gas flow, Discharge Glow, discharge Power output, Spindle rotation speed, depth of cut, Feed rate, Coolant [19]	Volume removal rate [10], Etching rate [10], Surface quality, Average surface roughness [19]
8	Plasma Chemical Vaporization Machining Process	Workpiece material, Atmospheric pressure plasma, Rf power, Chemical [30,66], Speed of etching, SF_6 : He ratio [30], He : CF_4 : O_2 ratio, Peripheral velocity [66]	Material Removal rate, Surface roughness [30,66]
9	Abrasive Diamond Wire Sawing Process	Workpiece material, Wire speed, Feeding speed, Tension force, Wire length [13]	Cutting force, Volume of material removal, Surface roughness [13]
10	Elastic Emission Machining Process	Workpiece material, Fine powder particles material, Diameter of fine powder particle, Volume concentration of particles in water, Temperature of fluid water, Gap of slit, Width of slit, Incident angle, Facing distance, Initial Velocity of fluid water, Removal depth, Removal area [20]	Surface roughness, Removal depths [20]
11	Abrasive Water Jet Machining Process	Workpiece material, Pump pressure, Focusing nozzle diameter, Abrasive flow rate, Jet impingement angle, Jet feed rate, Standoff distance [24]	Depth of erosion, Kerf geometry, Dimensional characteristics [24]

present graph shows that in 1995 up to 2004 the grinding process, laser machining process and sequential machining process are mostly used whereas, from 2005 up to recent days the development of SiC machining process is get increases due to the advancement in machining technologies.

4. SUMMARY

The SiC contains variety of properties due to which its applicability in various fields is increasing. But, it also includes some limitations i.e. long machining time, product reliability, low production rate, rapid

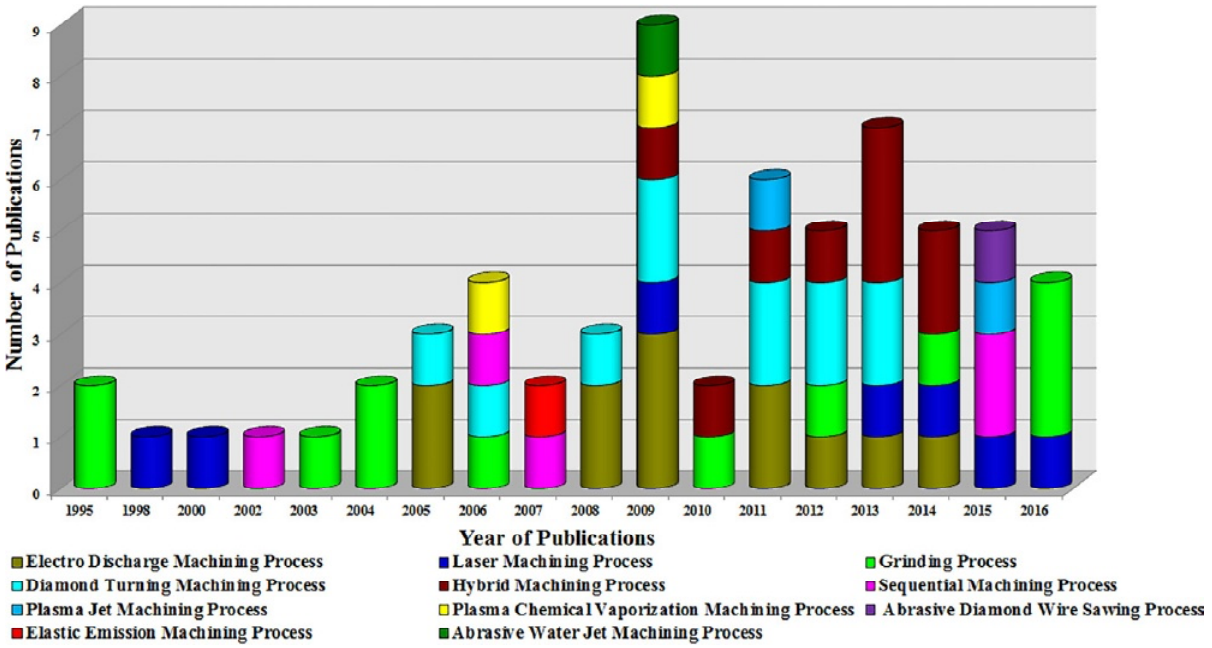

Fig. 2. Progress in machining processes of Silicon Carbide.

tool wear these all are responsible to make SiC machining very costly.

There are various processes used for machining of SiC, electro discharge machining process is one of them. It enhances MRR, hardness, mechanical character and surface quality. It gives significant results for high precision and high efficiency of SiC. It provides high pulse utilization and good machining stability. The conditions of positive tool polarity, high voltage, smaller high frequency, peak current, pulse duration and interval are the significant parameters for the machining of SiC. The water based emulsion gives high efficiency and good machining conditions during environmental practices of SiC. The material removal rate mechanism includes melting, evaporation and thermal spalling. The intensity and voltage are significant parameters for MRR. The flushing pressure, intensity, and pulse time affected the tool wear rate. The high MRR and Tool wear rate increases emulsion flux which decreases surface roughness. The high voltage drop causes instability during EDM of SiC. Hence to reduce this high voltage the workpiece wasted its energy part i.e. Joule heat. In EDM with the help of steel toothed wheel used as tool electrode a large surface area on SiC was obtained because it gives high MRR. However, the cutting speed of foil EDM for SiC was improved by taking copper foil as tool electrode.

The laser micromachining is another process used for SiC machining which contains various types of laser. In Local laser irradiation by using infrared laser with or without pre-heating causes ablation and thin films of SiC was removed. The increase in laser energy density decreases the depth of holes was observed in picoseconds laser pulses. The ablation threshold and absorption coefficient of SiC was successfully achieved in laser drilling process by using a single infrared 1064nm pulse laser. The underwater laser drilling of SiC by applying ns pulsed infrared Nd:YAG laser gives vias in which cracks, debris and heat affected zone are absent. The thermal effects in decomposing material, surface tension in expelling molten part, the effect of evaporation induced recoil pressure, loss in energy and cooling of the surface are responsible for the formation of hole in SiC drilling with A JK 701 pulsed Nd:YAG laser. The KrF excimer laser shows rugged surface morphology on SiC without cracks.

The diamond grinding wheel produces high MRR doesn't affecting surface morphology and finishing. During grinding performance of SiC the material properties of wheel and workpiece are important factor for predicting the surface roughness. In computerized numerical control grinding machine by utilizing metal bond diamond tools created the low induced damage. The micro-structural heterogeneity significantly increases the drilling and grinding rates of SiC. The increase in dynamic fracture toughness resulted into high MRR of SiC having better surface finish was achieved in high speed grinding process. In grinding methods by applying bonded abrasive wheels the low surface roughness and high shape accuracy achieved on mirrors of SiC. The combina-

tion of high workpiece speed and velocity of elevated grinding wheel can reduced the phase transformation observed during high speed cylindrical grinding process.

In single point diamond turning process the wear of diamond tool caused by sp3-sp2 order disorder transition. The numerical simulation results obtained by AdvantEdge software, helps to predict the thrust and cutting forces formed during ductile cutting condition which was caused by high pressure phase formed at cutting edge resulted into MRR. The ultra-precision diamond turning machine produces significant wear marks on cutting tool. The quantitative and qualitative behavior of this process shows higher thrust forces than the cutting forces. The improvement in tool performance and reduction in tool wear can significantly resulted by tool-swinging cutting method. A very high material removal rate was achieved by using large radius round nosed diamond tools in which cleavage cracking, ductile cutting and grain dislodgement showed precision machining. The precision machining and high material removal rate was successfully achieved by using single point diamond turning process.

The laser assisted machining process produced lower cutting forces which are important to reduce the tool wear. Whereas, the micro laser assisted machining process showed significant reduction in cutting forces. The hybrid process composed of end electrical discharge milling and mechanical grinding successfully machined the large surface area of SiC having a good surface quality. The higher grain penetration and more micro-pits were observed in ultrasonic vibration assisted grinding which resulted into slightly rougher ground surface. In carbon nanofiber assisted micro electro discharge machining process, the carbon nanofiber helps to enhance the electro discharge frequency, discharge gap, material removal rate and reduces the electrode wear and electrode tip concavity.

The cutting, lapping and polishing processes was sequentially applied for machining of large-diameter 6H-SiC wafers resulted into very smooth and low damage surface. The combination of non-traditional process and combined with deterministic finishing techniques produced low surface roughness on SiC. The mirror substrate of flat small diameter was achieved by sequential use of curve generation, grinding and polishing steps. Similarly, by using two stage fabrication processes i.e. polishing and lapping the reaction bonded SiC optical components with low surface roughness was achieved. The flat surface on optical and optoelectronic components was achieved by applying sequential polishing steps i.e. coarse polishing, pre-polishing, polishing and nano polishing.

The material removal rate of C-and Si-face of 4H-SiC were obtained by using excited plasma jet having atmospheric pressure of 13.56 MHz RF. The application of atmospheric pressure plasma jet offers high material removal rate, high surface quality and low surface roughness. The MRR is mainly depend on temperature in plasma chemical vaporization machining process hence, as etching temperature increases the increase in surface roughness was observed. Thus, as compared to Si face, the C face of SiC was etched faster resulted into very smooth surface with high machining rate. The abrasive diamond wire sawing process produced a sawn single crystal SiC surface with two areas i.e. fractured area and ploughing striations. The increased removal depth and smooth surface structure was achieved by using elastic emission machining process in which periodic step bunched structure exposed to the particles of silica powder. The abrasive water jet machining shows different erosion rates due to the enhanced erosion capacity of abrasive impact.

5. CONCLUSION

In this paper a review on machining processes of silicon carbide is presented. The research work carried out on SiC machining of last 20 years has been scrutinized. The specific focus has given to the input and output parameters of different machining processes used for SiC machining. Following are the some important conclusive remarks which are based on present overview.

The EDM process have good machining stability and high pulse utilization due to which it gives high removal rate, large machined area, high efficiency, good surface quality with low cost machining and good environmental conditions. The formation of micropores and micro cracks, heat loss and voltage drop are the limitations for EDM process. Whereas, the grinding process improves the productivity, surface quality and provides high removal rate, low surface roughness with high shape accuracy. The laser machining process formed rugged morphology with surface modification and ablation of surface depth. The underwater laser process gives SiC surface without debris and heat affected zone. Whereas, the laser process in air medium produces debris and particles. The CO_2 laser process produces toxic gases which are harmful to the environment. However, the single point diamond turning process offers excellent surface finish and

nanometric surface roughness. The most critical problem in this process is tool wear and wear marks on cutting tool.

In hybrid machining process, two machining processes are combined together and used for the machining of SiC. The combination of EDM and mechanical grinding process, machined large surface area with lower surface roughness and produces good surface quality having high MRR. It has high machining efficiency, low equipment cost and fine working environmental practice. While, the carbon nanofibre assisted electro discharge machining process improves the electrode tip concavity, electro discharge frequency, electrode wear, material removal rate, discharge gap and machinability. The ultrasonic assisted grinding process provides more stable grinding force with slightly rougher and good surface. The laser assisted diamond turning machining process enhances tool life and produces high productivity with higher material removal rate.

Thus, from the present review it can be said that the electro discharge machining process, grinding process, laser machining process, diamond turning machining process are the most efficient and widely used processes for the machining of SiC. As well as, the combination of these processes termed as hybrid machining is also given superior results and eliminates the limitations of individual process so this can also be the most suitable machining process for SiC. Hence, this study will help to quick referencing and selecting the most appropriate machining process for SiC which can be used for further research in SiC materials.

REFERENCES

[1] J. Roy, S. Chandra, S. Das and S. Maitra // *Rev. Adv. Mater. Sci.* **38** (2014) 29.

[2] R. Mahdavinejad, M. Tolouei-Rad, H. Sharifi-Bidgoli // *International Journal of Numerical Methods for Heat and Fluid Flow* **15** (2005) 483.

[3] D. Ravindra, S. Virkar and J. Patten // *Properties and Applications of Silicon Carbide, Ductile Mode Micro Laser Assisted Machining of Silicon Carbide (SiC), Chapter 1* (Intech Publisher, 2011)

[4] S. Goel, X. Luo, R.L. Reuben, W.B. Rashid and J. Sun // *Key Engineering Materials* **496** (2012) 150.

[5] A.R. Shayan, H.B. Poyraz, D. Ravindra, M. Ghantasala, J.A. Patten, In: *Proceedings of the ASME 2009 International Manufacturing Science and Engineering Conference, (ASME, 2009) Vol. **1**, p. 827.*

[6] S. Agarwal, P.V. Rao // *International Journal of Machine Tools & Manufacture* **50** (2010) 1077.

[7] Y. Aono, S. Ando and A. Hirata // *Precision Engineering* **43** (2016) 270.

[8] R. Ji, Y. Liu, Y. Zhang, F. Wang, B. Cai and H. Li // *Chinese science bulletin* **57** (2012) 421.

[9] K. Ding, Y. Fu, H. Su, X. Gong and K. Wu // *Int. J. Adv. Manuf. Technol.***71** (2014) 1929.

[10] I.M. Eichentopf, G. Bohm and T. Arnold // *Surface & Coatings Technology* **205** (2011) S430.

[11] S. Goel, X. Luo, P. Comley, R.L. Reuben and A. Cox // *International Journal of Machine Tools & Manufacture* **65** (2013) 15.

[12] A.V. Gopal and P.V. Rao // *Int. J. Adv. Manuf. Technol.* **24** (2004) 816.

[13] H. Huang, Y. Zhang and X. Xu // Int. J. Adv. Manuf. Technol. **81** (2015) 955.

[14] R. Ji, Y. Liu, L. Yu, X. Li and X. Dong // *Chinese Science Bulletin* **53** (2008) 3247.

[15] R. Ji, Y. Liu, Y. Zhang and F. Wang // *Int. Journal of Refractory Metals and Hard Materials* **29** (2011) 117.

[16] R. Ji, Y. Liu, Y. Zhang, X. Dong, Z. Chen and B. Cai // *Journal of Mechanical Science and Technology* **25** (2011) 1535.

[17] R. Ji, Y. Liu, Y. Zhang, B. Cai, J. Ma and X. Li // *Int. J. Adv. Manuf. Technol.* **59** (2012) 127.

[18] R. Ji, Y. Liu, Y. Zhang, B. Cai, X. Li and C. Zheng // *Journal of Mechanical Science and Technology* **27** (2013) 177.

[19] K. Katahira , H. Ohmori, S. Takesue, J. Komotori and K. Yamazaki // *CIRP Annals-Manufacturing Technology* **64** (2015) 129.

[20] A. Kubota, Y. Shinbayashi, H. Mimura, Y. Sano, K. Inagaki, Y. Mori and K. Yamauchi // *Journal of Electronic Materials* **36** (2007) 92.

[21] P.J. Liew, J. Yan and T. Kuriyagawa // *Journal of Materials Processing Technology* **213** (2013) 1076.

[22] Y. Liu, R. Ji, Q. Li, L. Yu and X. Li // *International Journal of Machine Tools & Manufacture* **48** (2008) 1504.

[23] X. Luo, S. Goel and R.L. Reuben // *Journal of the European Ceramic Society* **32** (2012) 3423.

[24] D.S. Srinivasu, D. A. Axinte, P.H. Shipway and J. Folkes // *International Journal of Machine Tools & Manufacture* **49** (2009) 1077.

[25] Q. Zhang, C. Wang, Y. Liu, L. Zhang and G. Cheng // *Journal of Wuhan University of Technology-Mater. Sci. Ed.* **30** (2015) 437.
[26] Y. Zhao, M. Kunieda and K. Abe // *Procedia CIRP* **6** (2013) 135.
[27] X. Chen, J. Li, D. Ma, X. Hu, X. Xu and M. Jiang // *J. Mater. Sci. Technol.***22** (2006) 681.
[28] Y. Wang, Y. Zhang and J. Han, *In: 2nd International Symposium on Advanced Optical Manufacturing and Testing Technologies (International Society for Optics and Photonics, 2006),* Vol. **6149**, p. 61490W-1.
[29] J.S. Johnson, K. Grobsky and D.J. Bray, In: *International Symposium on Optical Science and Technology* (International Society for Optics and Photonics, 2002), Vol. **4771**, p. 243.
[30] Y. Sano, M. Watanabe, T. Kato, K. Yamamura, H. Mimura and K. Yamauchi // *Materials Science Forum* **600-603** (2009) 847.
[31] Y.H. Liu, R. Ji, Q. Li, L. Yu and X. Li // *Journal of Alloys and Compounds* **472** (2009) 406.
[32] Z. Zhang, J. Yan and T. Kuriyagawa // *Int. J. Adv. Manuf. Technol.* **57** (2011) 117.
[33] T. Kato, T. Noro, H. Takahashi, S. Yamaguchi and K. Arai // *Materials Science Forum* **600-603** (2009) 855.
[34] J. Yan, Z. Zhang and T. Kuriyagawa // *International Journal of Machine Tools & Manufacture* **49** (2009) 366.
[35] L. Yin, E.Y.J. Vancoille, L.C. Lee, H. Huang, K. Ramesh, X.D. Liu // *Wear* **256** (2004) 197.
[36] S. Goel, X. Luo, R.L. Reuben and W.B. Rashid // *Nanoscale Research Letters* **6** (2011) 589.
[37] D.H. Duc, I. Naoki and F. Kazuyoshi // *International Journal of Heat and Mass Transfer* **65** (2013) 713.
[38] N. Iwatani, H.D. Doan and K. Fushinobu // *International Journal of Heat and Mass Transfer* **71** (2014) 515.
[39] R. Ji, Y. Liu, Y. Zhang, B. Cai, H. Li and J. Ma // *Int. J. Adv. Manuf. Technol.* **51** (2010) 195.
[40] N.P. Padture, C.J. Evans, H.H. Xu and B.R. Lawn // *J. Am. Ceram. Soc.* **78** (1995) 215.
[41] J.A. Patten and J. Jacob //*Journal of Manufacturing Processes* **10** (2008) 28.
[42] A.J. Damiao and M.V.R. Dos Santos, *In: Journal of Physics: Conference Series* Vol. **605** (IOP Publishing, 2015), p. 012001.
[43] H. Abderrazak and E.S.B.H. Hmida, In: *Silicon carbide: Synthesis and properties*. (INTECH Open Access Publisher, 2011), p. 363.
[44] M.B. Wijesundara and R. Azevedo, In: *SiC materials and processing technology. In Silicon carbide microsystems for harsh environments* (Springer New York, 2011), p. 33.
[45] Y. Pachaury and P. Tandon // *Journal of Manufacturing Processes* **25** (2017) 369.
[46] A.N. Samant and N.B. Dahotre // Journal of the European Ceramic Society **29** (2009) 969.
[47] S. Goel // *J. Phys. D: Appl. Phys.* **47** (2014) 243001.
[48] C.H. Lauro, L.C. Brandao, T.H. Panzera and J.P. Davim // *Rev. Adv. Mater. Sci.* **40** (2015) 227.
[49] C.J. Luis, I. Puertas and G. Villa // *Journal of Materials Processing Technology* **164–165** (2005) 889.
[50] F. Zeller, T. Hosel, C. Muller and H. Reinecke // *Microsyst. Technol.* **20** (2014) 1875.
[51] S. Yamaguchi, T. Noro, H. Takahashi, H. Majima, Y. Nagao, K. Ishikawa, Y. Zhou and T. Kato // *Materials Science Forum* **600-603** (2009) 851.
[52] A.N. Samant, C. Daniel, R.H. Chand, C.A. Blue and N.B. Dahotre // *Int. J. Adv. Manuf. Technol.* **45** (2009) 704.
[53] I. Shigematsu, K. Kanayama, A. Tsuge and M. Nakamura // *Journal of Materials Science Letters* **17** (1998) 737.
[54] D. Sciti, C. Melandri and A. Bellosi // *Journal of Materials Science* **35** (2000) 3799.
[55] A.V. Gopal and P.V. Rao // *Int. J. Adv. Manuf. Technol.* **22** (2003) 475.
[56] B.P. Grotha, S.M. Langan, R.A. Haber and A.B. Mann // *Ceramics International* **42** (2016) 799.
[57] Y. Liu, B. Li, C. Wu and Y. Zheng // *Int. J. Adv. Manuf. Technol.* **86** (2016) 799.
[58] Z. Zhong and T. Nakagawa // *Journal of Materials Processing Technology* **56** (1996) 37.
[59] D. Zhu, S. Yan and B. Li // *Computational Materials Science* **92** (2014) 13.
[60] J. Ni and B. Li // *Materials Letters* **89** (2012) 150.

[61] J. Patten, W. Gao and K. Yasuto // *Transactions of the ASME*, **127** (2005) 522.
[62] H. Tanaka and S. Shimada // *CIRP Annals - Manufacturing Technology* **62** (2013) 55.
[63] Z. Zhang, J. Yan and T. Kuriyagawa // *Key Engineering Materials* **389-390** (2009) 151.
[64] S.R. Virkar and J.A. Patten // *Journal of Manufacturing Science and Engineering* **135** (2013) 041003-1.
[65] S. Goel, W.B. Rashid, X. Luo, A. Agrawal and V.K. Jain // *Journal of Manufacturing Science and Engineering* **136** (2014) 021015-1.
[66] Y. Sano, M. Watanabe, K. Yamamura, K. Yamauchi, T. Ishida, K. Arima, A. Kubota and Y. Mori // *Japanese Journal of Applied Physics* **45** (2006) 8277.
[67] H.Y. Tam, H.B. Cheng and Y.W. Wang // *Journal of Materials Processing Technology* **192–193** (2007) 276.
[68] Y.D. Filatov, A.G. Vetrov, V.I. Sidorko, O.Y. Filatov, S.V. Kovalev, V. D. Kurilovich, M.A. Danil' chenko, T.A. Prikhna, A. I. Borimskii, A.M. Katsai and V.G. Poltoratskii // *Journal of Superhard Materials* **37** (2015) 48.
[69] H.H.K. Xu, N.P. Padture and S. Jahanmir // *J. Am.* Ceram. So*c.* **78** (1995) 2443.
[70] B. Bhattacharya, J. A. Patten and J. Jacob, In: *Proceedings of ASME 2006 International Conference on Manufacturing Science and Engineering*, **Parts A and B** (ASME, 2006), p. 1153.